Forest Ecology and Management 545 (2023) 121246

Contents lists available at ScienceDirect

Forest Ecology and Management

journal homepage: www.elsevier.com/locate/foreco

Integrating active fire behavior observations and multitemporal airborne laser scanning data to quantify fire impacts on tree growth: A pilot study in mature *Pinus ponderosa* stands

Aaron M. Sparks [a,*], Alistair M.S. Smith [a,b], Andrew T. Hudak [c], Mark V. Corrao [a], Robert L. Kremens [d], Robert F. Keefe [a]

[a] Department of Forest, Rangeland, and Fire Sciences, College of Natural Resources, University of Idaho, Moscow, ID 83844, USA
[b] Department of Earth and Spatial Sciences, College of Science, University of Idaho, Moscow, ID 83844, USA
[c] Rocky Mountain Research Station, USDA Forest Service, Moscow, ID 83843, USA
[d] Chester F. Carlson Center for Imaging Science, Rochester Institute of Technology, Rochester, NY 14623, USA

ARTICLE INFO

Keywords:
Fire
Fire effects
Fire behavior
Severity
LiDAR
Height growth
Conifers

ABSTRACT

Methods that integrate pre-, active-, and post-fire measurements to quantify fire effects across multiple spatial scales are needed to improve our understanding of ecological effects following fire and for informing natural resource management decisions that rely on post-fire growth and yield estimates. Given growth and yield modeling systems require tree level measurements to parameterize diameter and height distributions, effective datasets require both tree and stand level characterization. However, most stand-to-landscape scale fire effects studies use optical multispectral data (e.g., 30 m spatial resolution Landsat data) which are too coarse to quantify tree-level effects and is limited in its ability to quantify changes in forest structure. Most studies also fail to integrate active fire behavior observations, such as heat flux, limiting their ability to identify mechanisms of tree injury and mortality and/or predict fire effects. Combining active fire observations and structural measurements derived from multitemporal airborne laser scanning (ALS) data has been proposed to quantify fire effects on tree structure and growth but has yet to be tested. In this pilot study, we used a combination of fire behavior and heat flux metrics, including Fire Radiative Power per unit area (FRP: W m^{-2}) and Fire Radiative Energy per unit area (FRE: J m^{-2}), along with multitemporal field and ALS measurements to quantify fire intensity impacts on mature tree height growth. Prescribed fires were conducted in 2014 in thinned and unthinned mature *Pinus ponderosa* stands and plot-scale fire behavior and heat flux metrics were quantified using standard videography methods and tower-mounted infrared radiometers. Tree height growth was quantified using multitemporal field and ALS data and included pre-fire measurements and post-fire measurements up to eight years post-fire. Results show that trees exposed to the surface fire treatments had height growth that was less than unburned trees. The results also show that height growth 5–8 years post-fire is reduced in trees exposed to greater fire intensities, in terms of maximum FRP per unit area and rate of spread. There was no significant relationship between height growth and other fire behavior metrics (FRE per unit area, average flame length, flame residence time), although height growth decreased with greater FRE per unit area and increased with greater flame residence time. These findings, taken together with similar sapling-, mature tree- and landscape-scale studies, suggest that an integrated active-fire behavior and ALS-data approach may provide a quantitative, scalable method for assessing fire effects on tree structure and growth.

1. Introduction

A long-standing challenge in wildfire science is the integration of pre-, active-, and post-fire measurements to assess ecological effects across a range of scales (Kremens et al., 2010; Smith et al., 2016). Although many remote sensing studies focus on the characterization of

* Corresponding author.
E-mail addresses: asparks@uidaho.edu (A.M. Sparks), alistair@uidaho.edu (A.M.S. Smith), andrew.hudak@usda.gov (A.T. Hudak), mcorrao@uidaho.edu (M.V. Corrao), kremens@cis.rit.edu (R.L. Kremens), robk@uidaho.edu (R.F. Keefe).

https://doi.org/10.1016/j.foreco.2023.121246
Received 4 May 2023; Received in revised form 29 June 2023; Accepted 1 July 2023
Available online 9 July 2023
0378-1127/© 2023 Elsevier B.V. All rights reserved.

fuels or the assessment of post-fire ecological effects (e.g., "severity", Lentile et al., 2006), studies are limited that measure the active-fire behavior (Wooster et al., 2021) and few studies characterize the pre-fire fuels where modeling of the heat released during the fire could potentially be inferred (e.g., Lutz et al., 2018, 2020). Individual tree- to stand-scale assessments are important for natural resource managers as they can help with planning of prescribed fires, quantification of impacts to growth and yield, and identification of post-fire rehabilitation actions (Hessburg et al., 2015; Keefe et al., 2022). However, the quantification of fire impacts to individual trees and forest stands is particularly challenging as trees of differing species, sizes, and ages can have vastly different physiological, growth, and mortality responses to heat-induced damage from fire (Hood et al., 2018; McDowell et al., 2018; Smith et al., 2017; Sparks et al., 2017). Furthermore, heat flux incident on trees can be highly variable in space and time due to the heterogeneous nature of fire behavior (O'Brien et al., 2018; Sparks et al., 2017) and occlusion due to other tree branches and canopies (Mathews et al., 2016). Remote sensing can provide pre-, active-, and post-fire data at a range of scales, however, linking active fire measurements to changes associated with pre- and post-fire conditions at individual tree to landscape scales is not well studied (Sparks et al., 2018a), with most landscape-scale studies utilizing only pre- and post-fire data (e.g., Lentile et al., 2006; Morgan et al., 2014; Picotte et al., 2021). Given wildfire activity is projected to increase in many forested areas of the United States (Abatzoglou et al., 2021; Anderegg et al., 2022) and there is a recognized need for more prescribed fires to be used for reducing hazardous fuel loads (Hiers et al., 2020; Kolden, 2019; Prichard et al., 2021), quantitative methods that can assess fire effects from the tree to landscape scale are needed.

Most remote sensing assessments of fire effects have predominately used pre- and post-fire optical multispectral data from airborne and satellite sensors as certain visible and near-infrared wavelengths are sensitive to the loss of photosynthetically active vegetation and the presence of char and ash (Lentile et al., 2006; Morgan et al., 2014; Roy and Landmann 2005; Smith et al., 2005; Sparks et al., 2016). While fire effects assessments can provide objective information on canopy cover loss (Alonzo et al., 2017; McCarley et al., 2017a, b; Meng et al., 2018) and tree mortality (Furniss et al., 2020) they provide limited information on structural change and growth dynamics of surviving trees. Many studies rely on data from satellite sensors including those on the Landsat satellite series (30 m spatial resolution), which is too coarse to assess individual tree and/or small stand fire effects (e.g., Cocke et al., 2005; Furniss et al., 2020; Smith et al., 2016), limiting its utility for forest managers. Furthermore, similar spectral reflectance can be observed from pixels with widely different fire effects (Smith et al., 2005), such as tree mortality (Furniss et al., 2020), which can introduce significant error to these assessments. This issue largely arises from the fact that spectral reflectance from individual pixels is a mixture of dominant canopy and understory components and is challenging to separate without data that can characterize the vertical dimension of the forest (McCarley et al., 2017a). The issue is also in part because at the scale of a 30 m pixel, different mixtures of fire behavior impacts, from unburned to complete consumption can be present; especially in regions of the fire where fire intensity is generally lower as more consistent degrees of consumption occur in areas of higher fire intensity (Smith et al., 2005). High-spatial resolution imagery (e.g., $<$ 10 m) and structure-from-motion image processing can minimize this issue by isolating spectral reflectance from individual tree crowns (Bergmüller and Vanderwel, 2022; Hamilton et al., 2021), but these assessments still lack the ability to identify mechanisms of fire effects as the heat flux, or other metrics of fire intensity, are not typically measured.

Integrating active fire observations into fire effects assessments provides a way to identify mechanisms of tree injury and mortality and predict fire effects (Kremens et al., 2010; Smith et al., 2016; Wooster et al., 2021). Recent dose–response studies that subject trees to known levels (i.e., doses) of heat flux via surface fires have shown that post-fire physiology (including photosynthesis, chlorophyll fluorescence, and phloem and xylem function), post-fire morphology (including stem diameter and height growth), and mortality of several sapling species vary as a function of fire intensity measures like fire radiative energy per unit area, or the total radiative heat flux, hereafter referred to as FRE density (FRED: J m^{-2}) (Partelli-Feltrin et al., 2021, 2023; Smith et al., 2017; Sparks et al., 2016, 2023; Steady et al., 2019). Furthermore, Sparks et al. (2017) observed stem radial growth reductions in mature *Pinus ponderosa* as a function of increasing maximum fire radiative power per unit area, or the instantaneous radiative heat flux, hereafter referred to as FRP density (FRPD: W m^{-2}). Although there is often some confusion with the use of the density term, Wooster et al. (2021) remarked that usage of the terms FRED and FRPD are appropriate over FRE and FRP, respectively, when considering energy release at a localized scale whereas FRE and FRP should be used at regional to synoptic scales. Others have shown using Moderate Resolution Imaging Spectroradiometer (MODIS) sensor data on the Terra and Aqua satellites that net primary productivity within burned forests is reduced to a greater degree where the observed FRE and maximum FRP was greater (Sparks et al., 2018a). Taken together, these studies suggest that maximum FRP and FRE may provide scalable active fire metrics to assess and predict fire effects, however, several uncertainties remain. Limited FRP observations over the duration of a fire represents a major limitation, given a lower observation frequency, such as that from spaceborne sensors, typically results in a poorer characterization of the fire behavior (Freeborn et al., 2014; Giglio, 2007). Additionally, the limited studies evaluating mature trees represents a key knowledge gap considering older and larger trees have more fire-resistant features (e.g., thicker bark, deeper rooting depth, higher crown) than saplings (He et al., 2012; Keeley, 2012; Starker, 1934; VanderWeide and Hartnett, 2011). Most of these studies have evaluated short-term post-fire responses (e.g., $<$2 years), leaving longer-term responses relatively unknown.

Structure and growth measurements assessed using airborne scanning light detection and ranging (LiDAR), commonly referred to as airborne laser scanning (ALS), can help fill these knowledge gaps by providing three-dimensional data at multiple spatiotemporal scales. ALS has been widely demonstrated to provide accurate measurements of many forest structure attributes, including tree height and canopy cover, across large spatial extents (Næsset, 1997; Hyyppa and Inkinen, 1999; Lefsky et al., 1999; Smith et al., 2009; Sibona et al., 2016; Sparks and Smith, 2022). Studies that use direct tree height measurements have shown that high pulse density ALS ($>$8 ppm) can estimate tree height with lower error and bias than indirect field measurements (Corrao et al., 2022; Ganz et al., 2019; Wang et al., 2019). These measurements have enabled mapping of vegetation vertical structure, i.e., the three-dimensional distribution of vegetation branches and foliage. Multi-temporal ALS datasets have been used to assess forest structural changes over time, such as canopy cover and volume (Wulder et al., 2009; Alonzo et al., 2017; McCarley et al., 2017a, 2017b; Meng et al., 2018) and biomass consumption due to wildfires (Bright et al., 2022; Chasmer et al., 2017; McCarley et al., 2020, 2022). However, prior studies, with a few exceptions (e.g., McCarley et al., 2020), have failed to link active fire observations with observed structure changes, limiting their insight into connecting fire behavior with fire impacts on structure and growth of individual surviving trees. This is an important missing link as this information could help calibrate modeled post-fire tree growth in fire effects and earth system models (Smith et al., 2016) and provide improvements to how fire effects are integrated within forestry growth and yield models (Steady et al., 2019). There is a well-documented history of accurately measuring individual tree height growth over time using multitemporal ALS datasets (Hyyppa and Inkinen, 1999; Yu et al., 2004; Ma et al., 2018; Zhao et al., 2018). Using active fire observations and individual tree measurements from multi-temporal ALS data has been proposed to objectively quantify fire impacts on individual trees (Sparks and Smith, 2022), but to date has not been assessed.

The overall objective of this pilot study was to understand how

variable surface fire intensity impacts longer-term (~2–8 years post-fire) mature tree height growth as a means to improve assessments of post-fire tree growth and yield. To achieve this, we assess growth effects in mature *Pinus ponderosa* Dougl. ex Laws. (ponderosa pine) stands that were burned under controlled conditions in October 2014. A suite of common fire behavior metrics (flame length, rate-of-spread, flame residence time) and FRPD were acquired at plots systematically located throughout the stands. Pre- and post-fire height measurements at the same plots were acquired using a combination of field surveys and ALS acquisitions. Finally, relationships between fire behavior metrics and ponderosa pine height growth were assessed at the plot scale using regression modeling.

2. Study area and data

2.1. Study area and experimental design

This study was conducted in the University of Idaho Experimental Forest (UIEF), ~20 km north-east of Moscow, Idaho, USA (Fig. 1a). The UIEF is a mixed-conifer, multi-use forest with a diverse range of stand structure and composition. Dominant species include *Pseudotsuga menziesii* (Mirb.) Franco var. *glauca* (Beissn.) Franco (Douglas fir), *Abies grandis* (Douglas ex D. Don) Lindl. (grand fir), *Thuja plicata* Donn ex D. Don (western redcedar), *Larix occidentalis* Nutt. (western larch) and *Pinus ponderosa* Dougl. ex Laws. (ponderosa pine). The present study builds off an experiment conducted in 2014 in three even-aged *Pinus ponderosa*-dominated stands (Sparks et al., 2017; Lyon et al., 2018). The three stands were planted in 1982 following clearcut harvest and have understories dominated by *Physocarpus malvaceus* (ninebark) and *Symphoricarpos albus* (snowberry). Elevation across the three stands ranges from 880 to 950 m. The local climate is characterized by cool and wet winters and warm and dry summers. Mean summer temperature over the 1991–2020 period was 17.2 °C and mean summer precipitation was 81 mm (annual precipitation was 622 mm) (NOAA, 2022).

In June 2014, three ~40 × 150 m treatment strips were surveyed and marked in each stand (Fig. 1, Lyon et al., 2018; Sparks et al., 2017). Two of the strips (~2 ha of each stand) were mechanically thinned to a target spacing of 6 m and chipped using a CAT 320B excavator (Caterpillar Inc., Peoria, IL, USA) equipped with a boom-mounted, drum-style mastication head. After thinning, density of trees greater than 5 cm diameter at breast height (DBH) ranged from 366 to 491 trees ha^{-1} in the thinned strips and from 533 to 1066 trees ha^{-1} in the unthinned strips (Fig. 2). Basal area ranged from 10.5–19.9 m^2/ha in the thinned strips and ranged from 14.1–33.6 m^2/ha in the unthinned strips (Fig. 2). In the thinned treatment strips, surface fuel had high spatial variability with litter fuel load ranging from 0.2 to 2.3 kg m^{-2}, duff fuel load ranging from 1.0 to 8.3 kg m^{-2}, and downed woody debris load ranging from 1.5 to 14.5 kg m^{-2} (Sparks et al., 2017). Litter and duff depth ranged from 4.7 to 8.4 cm. In the unthinned strips, downed woody debris load ranged from 0.02 to 0.17 kg m^{-2} and litter and duff depth ranged from 2.3 to 7.2 cm. No harvest or thinning occurred in these stands after 2014. In October 2014, prescribed burns were conducted in half of each stand (Fig. 1a). During the burning operations, temperature ranged from 16 to 20 °C and relative humidity ranged from 26 to 52%. Surface winds ranged from 1.6 to 4.8 km h^{-1}. The stands were ignited using drip torches, with ignition lines separated by ~8 m.

2.2. Field inventory data

Prior to thinning treatments, eighteen 10 × 10 m inventory plots were established in each stand ($N = 54$) in January 2014 following a systematic sampling design (Fig. 1b). The corners of each plot were marked with permanent metal posts and all trees >5 cm in DBH within the plot were marked with uniquely numbered tags. All plots within a stand were oriented on a common azimuth and the upper-left corner of each plot was geolocated with a Trimble GeoXT global positioning system (Trimble Inc., Westminster, CO, USA), so that plots could be precisely located in a geographic information system. All marked trees were measured for DBH and stump diameter using a foresters' tape and crown base height and total height were measured using a TruPulse 360 laser rangefinder/hypsometer (Laser Technology Inc., Centennial, CO, USA). Following thinning treatments in June 2014, each plot was

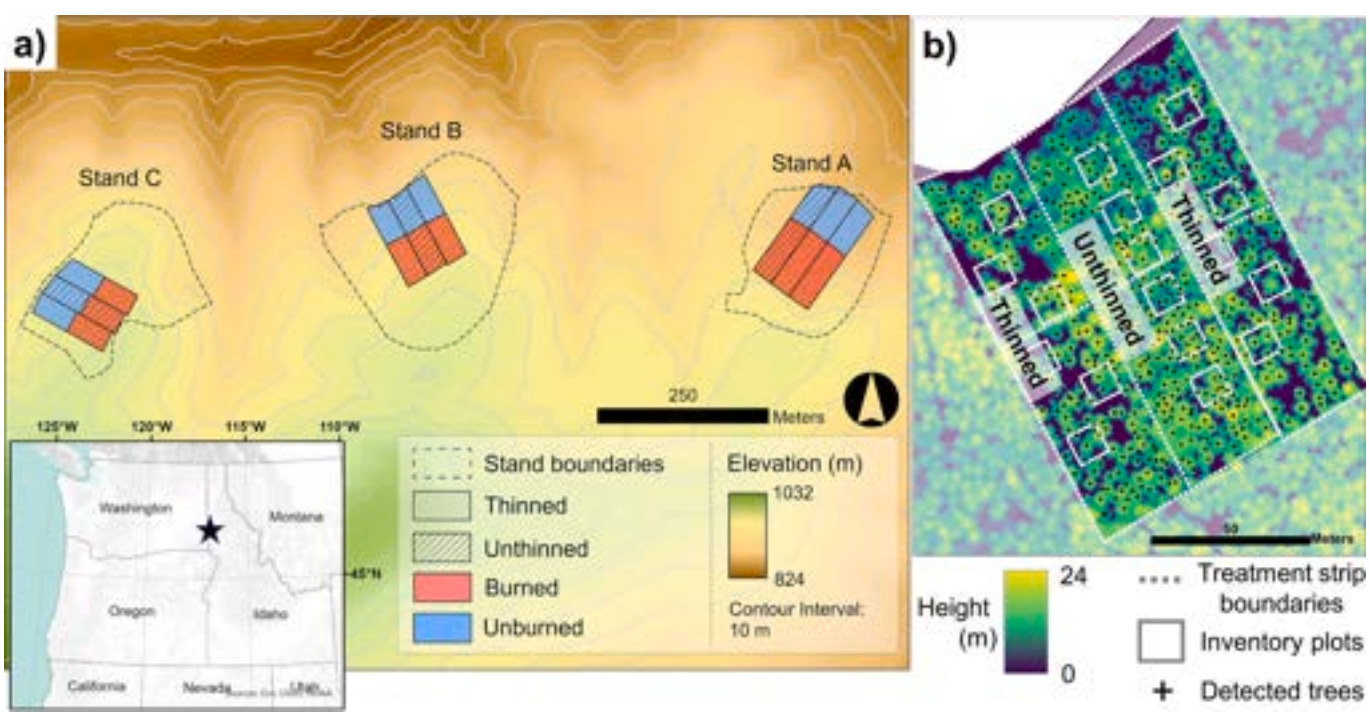

Fig. 1. Overview of the three study stands within the University of Idaho Experimental Forest study area in north-central Idaho, USA. a) Elevation and location of study treatments within each of the three stands. b) Canopy height model derived from the 2019 ALS data for Stand B. Treatment strip boundaries, matched individual trees, and forest inventory plot boundaries are overlayed.

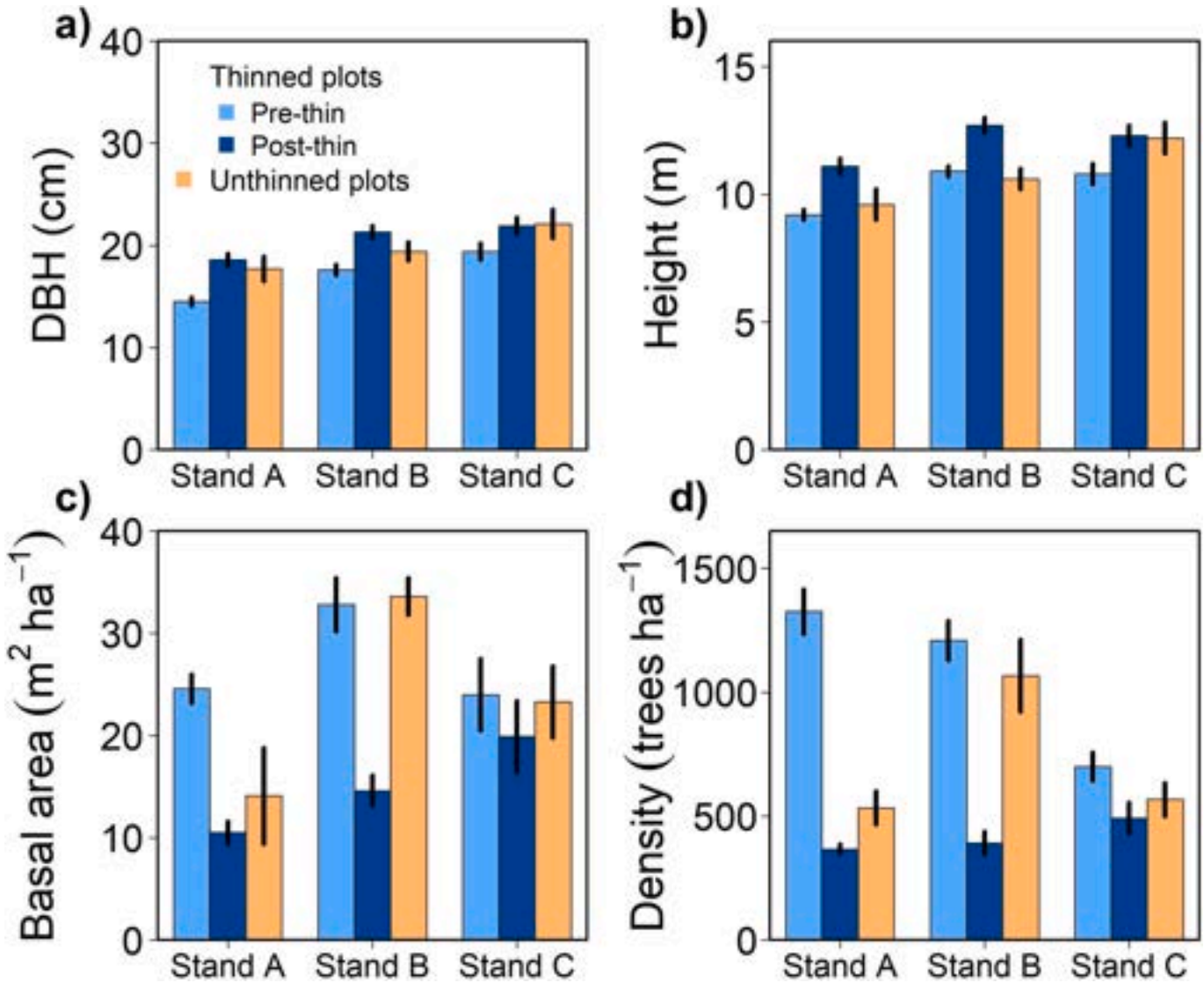

Fig. 2. Summary stand characteristics for thinned and unthinned treatment strips within the three study stands in 2014 (mean ± standard error). Subfigures show DBH (a), height (unweighted) (b), basal area (c), and tree density (d).

revisited and remaining trees in each plot were confirmed using the numbered tags. Tree measurement summary statistics for pre- and post-thinning in 2014 are presented in Fig. 2. In March 2016, DBH, total height and live/dead status were assessed on all remaining trees in the thinned treatments as part of a different study (Sparks et al., 2017).

2.3. Fire behavior measurements

Fire behavior measurements acquired during the October 2014 prescribed fire treatments are described in detail in Sparks et al. (2017) and Lyon et al. (2018) and a brief description is given here. Fire behavior was assessed in 5 × 7 m plots nested within nine of the forest inventory plots. Prior to burning, plot corners were marked with pin flags and a pole with graduated markings was placed at the center of each plot to serve as reference points. Plots were ignited on the downslope edge using a drip torch to establish a uniform flaming front. Video cameras (Samsung HMX-F90 HD Camcorder, Samsung Electronics America Inc., Ridgefield Park, NJ, USA) were positioned outside each plot so that corner pin flags and center pole were visible. Video was used to estimate the rate-of-spread of the fire front between the different reference points. Average flame length was estimated using still-frame video data, analyzed at 10-s intervals. Flame length is defined following Johnson (1992), where flame length is the distance from the center of the burning surface to the tip of continuous flame. Video was also used to estimate flame residence time, or the total time that plots maintained continuous flaming combustion (Cheney, 1990).

FRPD was measured using tower-mounted, dual-band infrared radiometers as described in Sparks et al. (2017). Radiometers were only deployed on plots in the thinned treatments due to concerns of potential damage resulting from intense fire behavior in the unthinned treatments. Details on sensor calibration and FRPD derivation using dual-band thermometry can be found in Kremens et al. (2010, 2012). The radiometers were mounted 5.2 m above the center of each plot (Fig. 3a, b) and recorded data at 0.1 Hz from pre-ignition to fire extinction. FRED was calculated as the temporal integral of FRPD observations. Maximum FRPD (kW m^{-2}) was identified as the maximum value of FRPD observations greater than zero over the burn duration. Average FRPD per unit time (FRPDμ: J m^{-2} h^{-1}) was calculated by dividing FRED by the total burn duration for a unit area. Total burn duration was calculated as the duration where FRPD was greater than zero.

2.4. Airborne laser scanning data and preprocessing

Three ALS datasets were used in this study, with all three completely

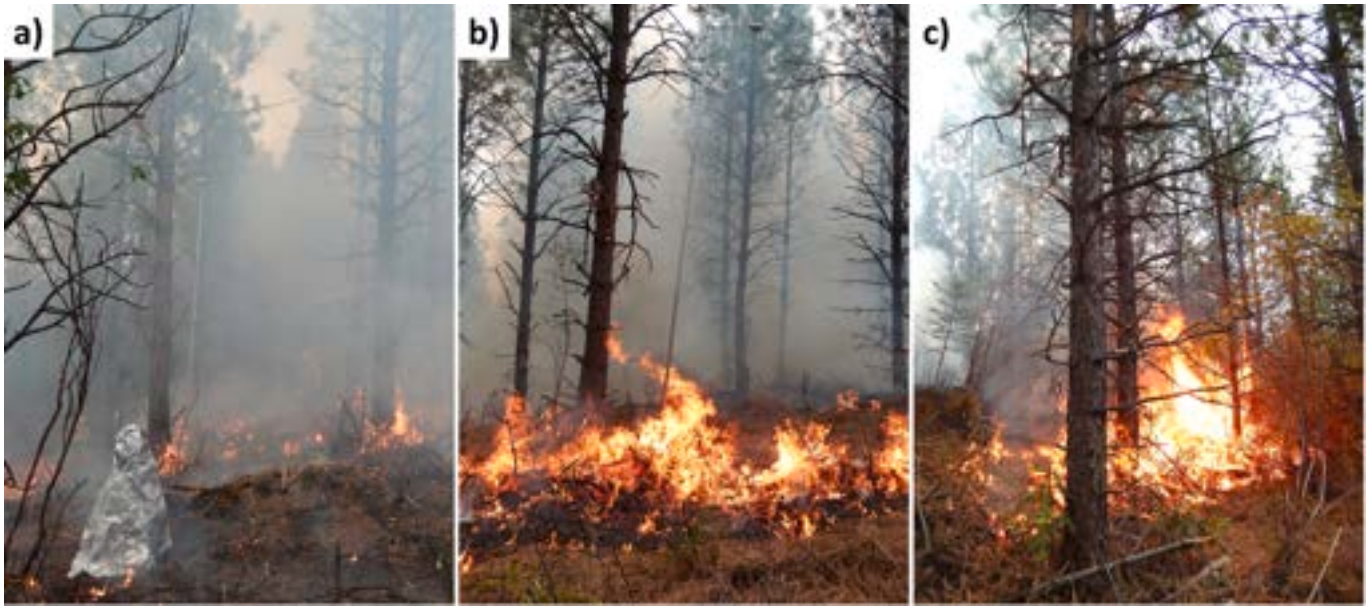

Fig. 3. Three example plots that illustrate the heat-shielded video camera and tower-mounted, dual-band infrared radiometer setup (a, b) and range of observed fire behavior across the three study stands (a, b, c). Average flame length was 0.3 m in (a), 1.5 m in (b), and 3 m in (c).

encompassing the three study stands. Acquisition parameters for the three ALS datasets are presented in Table 1. The first ALS dataset was acquired across the study area in July 2019 using a Teledyne Geospatial Optec Galaxy PRIME sensor (Teledyne Geospatial, Toronto, ON, Canada) mounted on a fixed wing aircraft. The sensor has a 60-degree field-of-view and elevation of the aircraft varied between 3550 and 4200 m above ground level to achieve a 50% flight-line overlap. Average pulse density was 8 pulses per square meter and the average per-pulse return rate over forested areas was two. The data were preprocessed by the supplier, which included classification of returns as bare earth and vegetation following the 2019 United States Geological Survey 3D elevation program (3DEP) specification (USGS, 2019).

The second and third ALS datasets were acquired across the study area in September 2020 and July 2022 using a RIEGL VQ-1560II sensor (RIEGL Laser Measurement Systems, Horn, Austria) mounted on a fixed-wing aircraft with a gyro-stabilized mount. The sensor has a 58-degree field-of-view and elevation of the aircraft varied between 1600 and 1900 m above ground level to achieve a 55% flight-line overlap. Average pulse density for both acquisitions was 20 pulses per square meter and the average per-pulse return rate over forested areas was four. Preprocessing conducted by the supplier consisted of laser intensity normalization using the RIEGL RiPROCESS software and return classification into bare earth, vegetation, water, buildings, and noise following the American Society for Photogrammetry and Remote Sensing classification standard (ASPRS, 2011).

Table 1
Acquisition specifications of the three ALS datasets.

Acquisition year	2019	2020	2022
ALS system	Teledyne Geospatial Optec Galaxy PRIME	Riegl VQ-1560II	Riegl VQ-1560II
Acquisition month	July	September	July
Flight altitude	3550–4200 m	1600–1900 m	1600–1900 m
Swath overlap	50%	55%	55%
Average pulse density	8 pulses m^{-2}	20 pulses m^{-2}	20 pulses m^{-2}
Average number of returns per pulse	2	4	4
Sensor field-of-view	60°	58°	58°

3. Methods

3.1. Individual tree detection and matching

Individual tree detection was conducted on each of the three ALS datasets using ForestView® ITD processing software described previously in Corrao et al. (2022), Sparks et al. (2022), and Sparks and Smith (2022). ForestView® is an ALS-based ITD software developed by Northwest Management Incorporated (NMI, Moscow, Idaho, USA) that provides individual tree location, height, DBH, stem volume, live/dead status and estimates of species. This approach uses the classified ALS point clouds to generate a high-resolution (0.3 m spatial resolution) digital elevation model and a digital surface model from which a canopy height model (CHM) can be derived. Peaks in the CHM are assumed to be treetops and are detected using several CHM- and point cloud-based ITD methods, similar to algorithms using valley following, watershed segmentation, and local max filtering. Structure related metrics (e.g., height percentiles, stratified return densities, crown shape) are used to refine the original tree detections and derive other tree attribute information (Corrao et al., 2022). Assessments of ForestView® ITD and height accuracy using data from the UIEF demonstrated that the method was able to identify most dominant trees (70% detected on average) and codominant trees (54% detected on average) across a wide range of stand densities (19–1847 trees ha^{-1}) (Sparks and Smith, 2022; Sparks et al., 2022). Regression-based equivalence tests indicated that paired field-measured height and ALS-derived height were statistically equivalent and that height RMSE was low (Sparks et al., 2022).

Following individual tree detection, a semi-automatic method was used to match the individual trees between the different ALS datasets. For each detected tree in the 2019 ALS dataset, candidate matching trees in the 2020 ALS dataset were selected if they were within 2.5 m of the detected tree, a distance that represents the average crown diameter of dominant and codominant trees on the UIEF (Falkowski et al., 2008). Next, the Euclidean distance and difference in height between each candidate tree and the 2019 detected tree were calculated. Candidate 2020 trees were not considered for a match if their height difference with the 2019 detected tree was greater than 2 m. This height difference threshold accounts for the average annual height growth observed on the UIEF of 0.4 m yr^{-1} (Hudak et al., 2012) and observed RMSE (0.69 m) in ALS-derived height (Sparks and Smith, 2022). Finally, the candidate

2020 tree with the smallest combined error (E) was matched with the 2019 detected tree using Eq. (1):

$$E = \sqrt{(x_1 - x_2)^2 + (y_1 - y_2)^2 + (h_1 - h_2)^2} \quad (1)$$

where (x_1, y_1) are the spatial coordinates and h_1 is the height of a treetop in one ALS dataset and (x_2, y_2) are the spatial coordinates and h_2 is the height of a treetop in a second ALS dataset. This matching process was repeated using the 2019 and 2022 ALS data. Gross matching errors were corrected by manually assessing the matched trees in a GIS along with each year's CHM and high-resolution imagery as reference data. Only trees that were matched between the three ALS datasets and within the forest inventory plot boundaries were used in the following analyses.

3.2. Tree height growth analysis

To quantify relationships between fire behavior and height growth, a preliminary screening was first employed to reduce errors and inconsistencies in the datasets. Ten plots that were dominated by species other than *Pinus ponderosa* were excluded from the following analysis, as most of these plots were unburned. Additionally, two plots that were crossed by fire containment lines and one plot that had changes independent of the prescribed fires (e.g., tree in plot falling between 2019 and 2022 ALS acquisitions), as assessed using the ALS-derived CHMs, were also excluded. High-resolution Google Earth imagery acquired in 2015 and 2022 was inspected to confirm that none of the trees in the plots died between 2014 and 2022, as evidenced by brown or defoliated crowns. After screening the final dataset used for analysis included 197 individual trees in 41 plots.

Height change for the remaining 197 trees was assessed using both the field- and ALS-derived height data. Individual tree heights for any given year were averaged to the inventory plot scale, as field data were not stem-mapped and trees could not be linked individually to the ALS-detected trees. Normalized height change, or relative height, was used to quantify differences in height growth among the treatments and fire behavior plots. Post-fire average height was normalized to pre-fire height to account for pre-fire differences in height among the inventory plots. Specifically, normalized height change for each post-fire height assessment year (t) was calculated following Eq. (2):

$$relative\ Height\ (\%) = \frac{(Height_t - Height_{prefire})}{Height_{prefire}} \quad (2)$$

Differences in relative height between treatments (unthinned and unburned, unthinned and burned, thinned and unburned, thinned and burned) were compared with ANOVA, and if significant ($\alpha = 0.05$), a Tukey's honest significant difference test.

We used pairwise ordinary least squares (OLS) regression to quantify the relationship between each fire behavior metric and relative height growth, where relative height growth was the dependent variable and fire behavior metrics were the independent variables. The coefficient of determination (r^2) and residual standard error were computed and used to evaluate the relationship 'goodness of fit'. We used the regression analysis slope to examine the magnitude and direction (positive or negative relationship) of impact that fire behavior had on relative height growth.

4. Results

Fire behavior in the October 2014 prescribed fires had high spatial variability and ranged from low rate-of-spread, smoldering dominated combustion to high rate-of-spread, high flame length fire fronts (Fig. 3). Flame lengths varied from 0.3 to 3 m, rate of spread ranged from 0.27 to 6 m min^{-1}, and flame residence time ranged from 0.08 to 0.37 h (Sparks et al., 2017). Maximum FRPD observations ranged from 1.7 to 16.3 kW m^{-2}, FRPDμ ranged from 0.04 to 0.9 MJ $m^{-2}h^{-1}$, and FRED ranged from 0.17 to 9.8 MJ m^{-2}. Some plots experienced very active fire behavior (e.g., high flame length and single tree torching), however, on average, smoldering-dominated combustion accounted for ~ 97% of the total burn duration (Sparks et al., 2017).

The mean height across all study trees increased from 12.5 (±0.2) m in 2014 to 16.4 (±0.1) m in 2022 (Fig. 4). This average height increase of ~3.9 m in 8 years equates to a growth rate of 0.48 m per year. Height increased an average of 0.74 (±0.02) m from 2019 to 2020 and 0.52 (±0.01) m from 2020 to 2022.

Relative height growth varied by thinning treatment and burn treatment. Although not significantly different ($P > 0.05$), trees in unburned plots experienced greater relative height growth than burned plots (Fig. 5). On average, relative height growth was 2.7% greater in unthinned, unburned plots than unthinned, burned plots. Likewise, relative height growth was 3.3% greater in thinned, unburned plots than thinned, burned plots. Relative height growth was greater in unthinned plots versus thinned plots (Fig. 5). On average, relative height growth in unthinned, unburned plots was 10.5% greater than thinned unburned plots. Likewise, relative height growth was 13.1% greater in unthinned, burned plots than thinned, burned plots.

Relative height in 2022 decreased linearly with increasing $FRPD_{max}$ ($P < 0.01$) (Fig. 6a) and rate of spread ($P < 0.05$) (Fig. 6e). These relationships were also observed for 2019 and 2020 relative height ($P < 0.01$), but not for 2016 ($P > 0.05$). There were no significant relationships between relative height and FRPDμ, FRED, average flame length, or flame residence time using any of the four post-fire datasets. Although not statistically significant ($P > 0.05$), relative height in 2019, 2020, and 2022 decreased with increasing FRED (Fig. 6c) and increased with greater flame residence time (Fig. 6f).

5. Discussion

This pilot study linked pre- and post-fire tree height measurements assessed via field and ALS data with fire behavior and heat flux to quantify fire behavior impacts on mature tree height growth at the plot scale. We show that height growth is reduced in mature *Pinus ponderosa* exposed to surface fires with greater maximum FRPD and rate of spread. Importantly, the persistence of this effect (up to 8 years post-fire) indicates longer-term fire impacts on tree growth and yield, even for relatively low-intensity surface fires like those employed in this study.

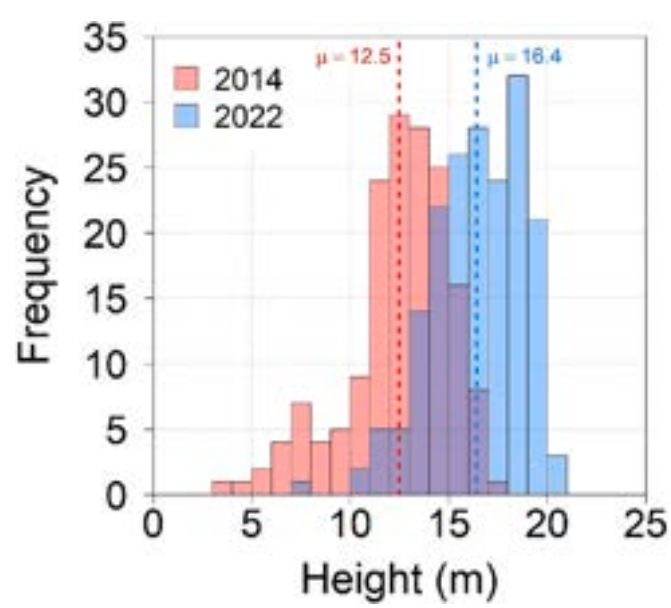

Fig. 4. Height distribution shift of all study trees from 2014 (red) to 2022 (blue). Purple coloration indicates where distributions overlap, and dashed lines mark the mean value for each distribution.

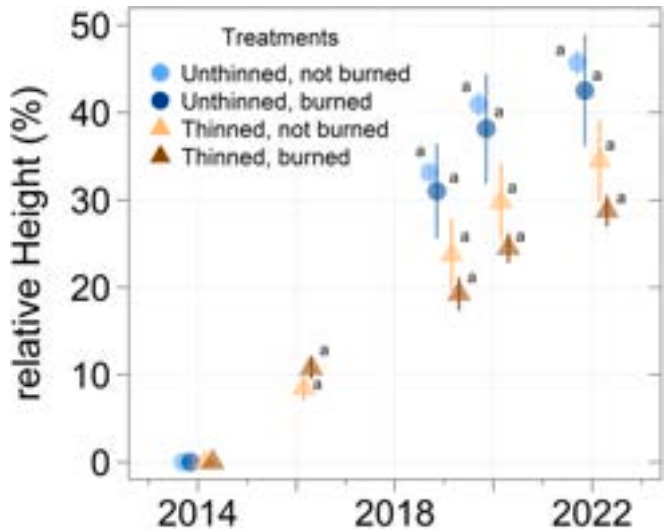

Fig. 5. *Pinus ponderosa* relative height (%, mean ± SE) at the plot scale from 2014 to 2022 by treatment. Mean values sharing the same letter for the same year are not significantly different ($P < 0.05$). Markers are slightly offset from the corresponding x-axis year for visibility purposes.

These findings also suggest that remotely sensed measures of fire behavior, such as maximum FRPD, can potentially provide a scalable active fire metric to assess and predict fire effects. This is important as FRP observations are currently acquired via sensors on multiple platforms including airborne (e.g., Hudak et al., 2015; Schroeder et al., 2014a) and satellite platforms (Giglio et al., 2016; Schroeder et al., 2014b) and could support the quantification of fire effects at scales ranging from individual trees to regions (Bowman et al., 2017). When considered with prior results showing stepwise decreases in stem diameter growth with increasing FRPD (Sparks et al., 2017), the methods outlined in this study highlight a way to quantify and predict fire impacts on tree growth and yield and serve as a useful planning tool for managers to gauge productivity reduction due to wildfires and prescribed fires (Keefe et al., 2022; Smith et al., 2017).

Numerous studies have assessed the ability of single-date and multitemporal ALS data to quantify fire effects on forest structure. McCarley et al. (2017a,b) used pre- and post-fire ALS datasets and Landsat optical data to quantify canopy cover change across the 2012 Pole Creek Fire in mixed coniferous forest in Oregon, USA. Likewise, Alonzo et al. (2017) used pre- and post-fire ALS and Landsat data to quantify fire-induced changes in canopy volume in mixed conifer-broadleaf forest in Alaska, USA. Meng et al. (2018) used single-date ALS data and multitemporal high-resolution multispectral imagery to quantify canopy cover loss and recovery in burned mixed pine-oak forest in New York, USA. An advantage of many of these prior studies is that they relate ALS-derived structural change with freely accessible optical data such as Landsat. This provides a route for researchers and managers with limited access to ALS data to quantify structural effects, such as canopy cover loss, in an objective manner. However, methods that use ALS data scaled to common moderate resolution optical data (e.g., 30 m Landsat data) may have limited utility for forest managers as this resolution is too coarse to assess individual tree and/or small stand fire effects (e.g., Cocke et al., 2005; Furniss et al., 2020; Smith et al., 2016). A major limitation of prior studies is that most do not incorporate active fire behavior data such as

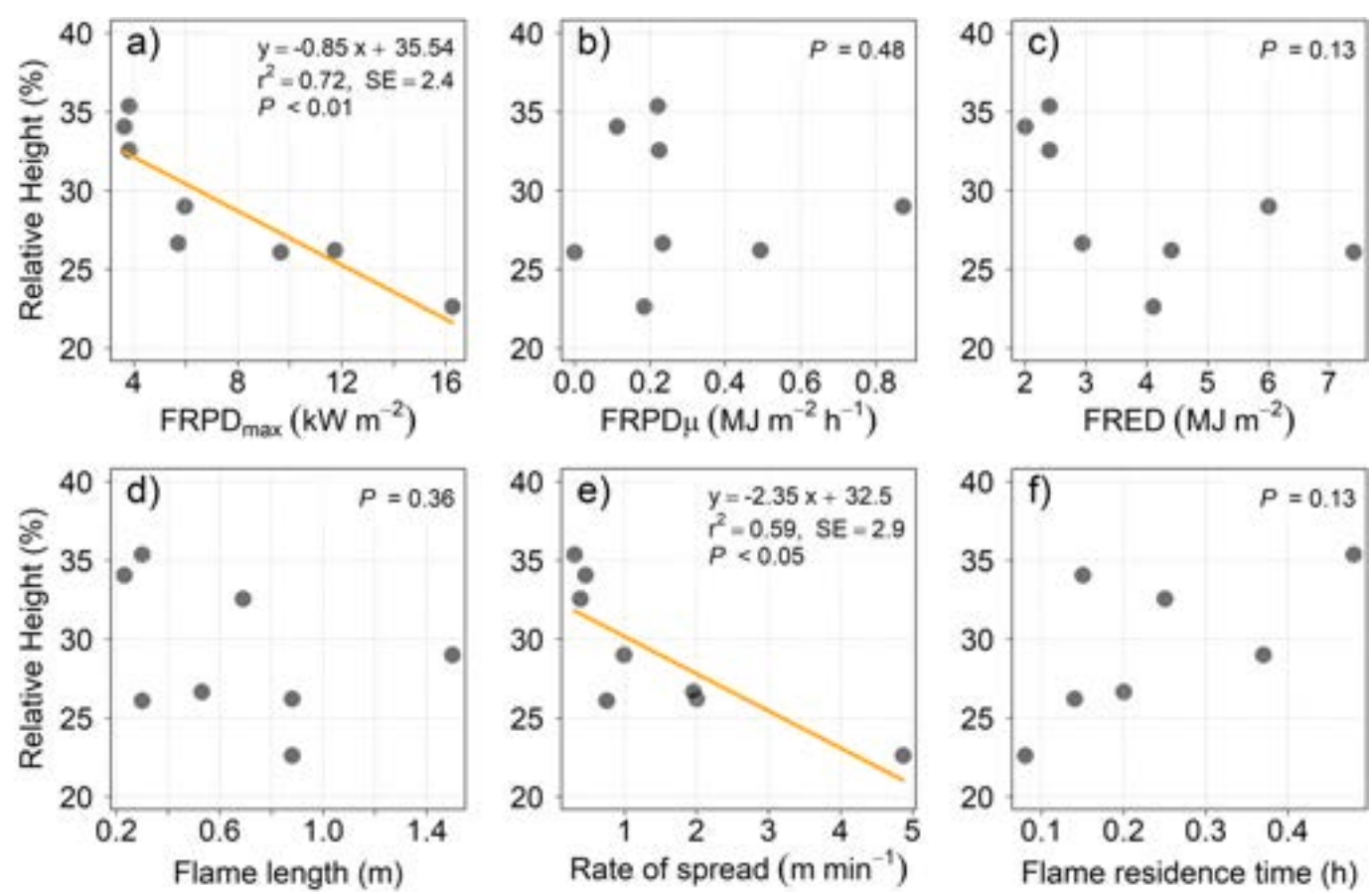

Fig. 6. Relationships between relative height in 2022 at the plot scale and fire behavior metrics including: $FRPD_{max}$ (a), FRPDμ (b), FRED (c), flame length (d), rate of spread (e), and flame residence time (f). The regression P-value (*P*) is displayed in all panes. The regression fit (orange line), r^2, and residual standard error (SE) is displayed for statistically significant relationships ($\alpha = 0.05$).

FRP and FRE, limiting their ability to build predictive models between fire intensity and structural change, such as post-fire canopy cover and height growth. An exception is McCarley et al. (2020), who quantified the relationship between MODIS-derived FRE with ALS- and field data-derived surface and canopy fuel consumption in two mixed coniferous forests. Quantifying this relationship is important as it means that MODIS-derived FRE could potentially be used to estimate surface and canopy fuel consumption in similar forests where ALS/field data are not available.

A primary advantage of the methods used in the present study is the incorporation of remotely sensed fire intensity data, which could be used to derive predictive models of post-fire tree growth and structure change for application across large spatial extents. The results suggest that active fire observations such as FRP could potentially be used to predict productivity reductions within forests and stands and help inform management decisions including harvesting scheduling and/or thinning severely injured and slow-growing trees after fire. Equally, these relationships could be used to parameterize existing growth and yield models that are typically used at the stand scale, such as the Forest Vegetation Simulator (Rebain, 2015). A disadvantage of using methodology that incorporates active fire observations is that moderately high temporal frequency active fire observations are required to adequately characterize fire behavior dynamics. Due to the high spatial and temporal heterogeneity of fire behavior, a lower observation frequency can result in a poorer characterization of the fire behavior (Freeborn et al., 2014; Giglio, 2007; Hudak et al., 2015). Modeling fire intensity could potentially be used in situations where active fire observations are not available (Lutz et al., 2018; 2020).

The finding that mature trees exposed to higher intensity surface fire exhibit lower growth rates is consistent with prior observations. For example, Landsberg et al. (1984) observed height growth in *Pinus ponderosa* exposed to more intense fire behavior (flame lengths: 0.6–1 m) that was 18% lower than unburned trees and smaller growth reductions (8% lower than unburned trees) in trees exposed to fire with less intense fire behavior (flame lengths: 0.3–0.5 m). We also observed that growth varied with $FRPD_{max}$ and rate of spread (Fig. 6a, e) but not with FRPDμ or FRED (Fig. 6b, c). Although not statistically significant, relative height declined with increasing FRED and average flame length (Fig. 6c, d). These observations are similar to the findings in Sparks et al. (2017) who found that *Pinus ponderosa* stem diameter growth decreased with increasing $FRPD_{max}$ but not FRPDμ or FRED. Taken together, we hypothesize that this discrepancy is resulting from greater damage to the tree crown due to convective heat fluxes. Prior studies that have shown FRP is positively related with convective heat flux (Freeborn et al., 2008; Finney et al., 2015). Greater damage in the tree crown would likely reduce photosynthesis in damaged foliage (Smith et al., 2017; Sparks et al., 2018b) and potentially cause trees to shift resources toward tissue repair rather than growth. Plots with the highest FRED also tended to be dominated by smoldering combustion and likely a heat dose distributed over a longer period of time. It is also notable that the relationship between $FRPD_{max}$ and height growth was only significant for years after 2016. The lack of relationship in 2016 may be partially owing to the extremely hot and dry growing conditions between pre-fire (2014) and field measurements in 2016. In 2015, the summer temperature was 3.5 °C greater than the average observed from 1991 to 2020 and summer precipitation was 16% of normal (NOAA, 2022). Given these abnormally hot and dry conditions, it is likely that all trees, even unburned trees, exhibited very limited growth. For the remaining years in the study time period (2016–2022), the summer temperature was 1.8 °C greater, on average, than the average observed from 1991 to 2020 and the summer precipitation was 70%, on average, of normal (NOAA, 2022).

While a field-to-ALS height measurement comparison could not be undertaken as measurements were acquired on different years, there are several lines of evidence that suggest that the growth observed in this study is accurate. Firstly, several accuracy assessments have been conducted using the same ALS datasets in this study. Sparks and Smith (2022) and Sparks et al. (2022) validated ALS-derived height (derived from 8 ppm and 20 ppm data) using 67 fixed radius field-measured inventory plots using regression-based equivalence tests and found that paired field-measured and ALS-derived height were statistically equivalent. The relationship between field-measured and ALS-derived height also had high r^2 (0.99) and low RMSE (0.69 m). Furthermore, others have validated both field and ALS height measurements using felled tree or high precision terrestrial laser scanning measurements and found that high return density (e.g., >12 points m^{-2}) ALS-derived height typically has lower RMSE and bias compared to field-measured height (Corrao et al., 2022; Ganz et al., 2019; Wang et al., 2019). Secondly, the average growth rate observed in this study (0.48 m per year) is similar to growth rates others have observed in the local region. Hudak et al. (2012) reported an annual growth rate of 0.4 (±0.8 s.d.) m per year across a range of species, stand ages and structures within a local area on the UIEF. Likewise, annual growth rates of 0.2–0.6 m per year for *Pseudotsuga menziesii* var. *glauca* have been observed in the UIEF and surrounding region (Hemingway and Kimsey, 2020).

We observed greater relative height growth in unthinned versus thinned trees, which while rare, has been observed in prior studies. Qiu et al. (2021) used height-diameter allometry data from plots across the western United States to show that *Pinus ponderosa* invest more resources in height versus diameter in stands with higher tree density. Greater height growth of trees in denser stands has also been observed in other species including *Pinus sylvestris* L. (Mäkinen and Isomäki, 2004; Tymińska-Czabańska et al., 2022) and *Populus tremula* L. × *P. tremuloides* Michx. (Lee et al., 2021). Reduced growth in thinned stands has been hypothesized to result from thinning shock, where thinned trees display chlorotic foliage and sunscald when shaded leaves are exposed to full sunlight (Harrington and Reukema, 1983; Simonin et al., 2006). Thinned trees can also display differing resource allocation patterns than unthinned trees, for example allocating more resources to crown diameter and root system growth than to height growth (Poorter et al., 2012). Ma et al. (2018) used multitemporal ALS data to characterize tree height and crown diameter growth and observed that trees in less dense stands exhibited greater crown diameter growth than trees in denser stands. Likewise, the trees in the thinned treatments of this study also displayed greater crown diameter expansion than unthinned trees from 2019 to 2022. Fig. 7 shows that crown edges in thinned treatments exhibited increases in height from 2019 to 2022, implying crown diameter expansion. These differences in growth are captured by increases in canopy cover, or the proportion of CHM cells within each treatment greater than 2 m in height (Alonzo et al., 2017). Canopy cover in unthinned treatments increased 2% on average, from 93% in 2019 to 95% in 2022, whereas canopy cover in thinned stands increased 7% on average, from 75% in 2019 to 82% in 2022.

While the results observed in this pilot study highlight a promising approach for assessing fire effects, this study was limited to a relatively small number of individuals of one conifer species. Given *Pinus ponderosa* is considered a fire-resistant tree at maturity (Keeley, 2012; Starker, 1934), approaches like this study could be used to evaluate the effects of fire behavior on growth for other species, size classes and life stages. Other opportunities for using a paired FRP-multitemporal ALS approach include the identification of mortality dose–response curves for different species and size classes of trees as well as mapping of trees killed by fire. ALS return intensity has been used previously to estimate dead tree density (Martinuzzi et al., 2009), however, its application to fire induced mortality has not been explored. Studies have shown that spectral reflectance at near-infrared wavelengths commonly used in ALS systems can characterize physiological function and mortality at the tree crown scale (Sparks et al., 2016). Considering ALS-guided high-resolution imagery has been used successfully to quantify physiology, water content, and chemical content of individual tree crowns (Asner et al., 2015), future work could evaluate the ability of multi-sensor data for crown-level stress and mortality assessments after fire. Paired FRP-multitemporal ALS approaches could further be useful for assessing

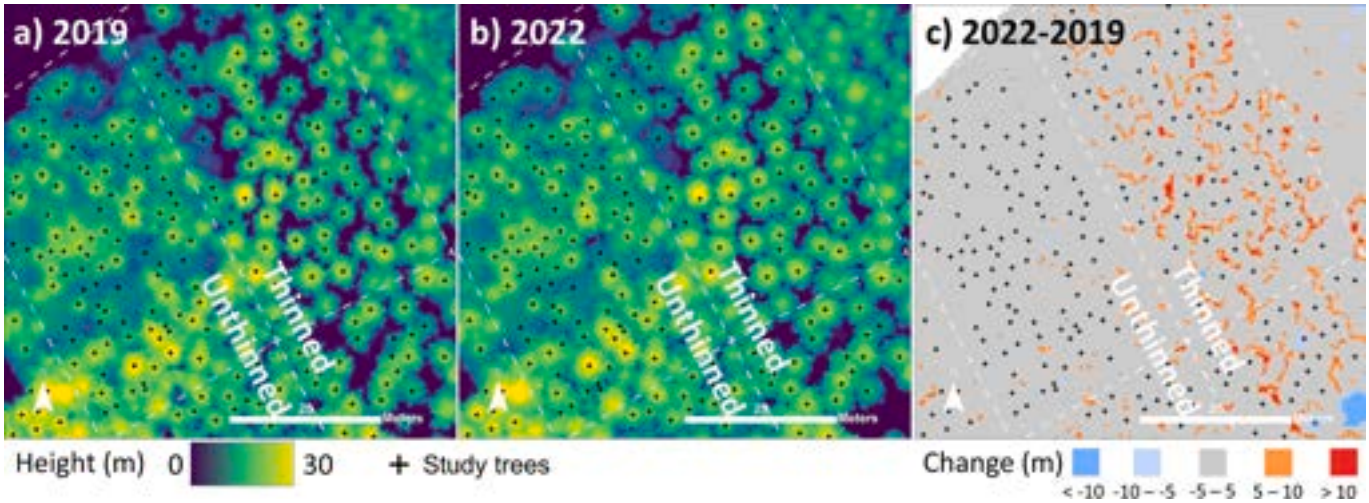

Fig. 7. ALS-derived canopy height models in Stand B for 2019 (a), 2022 (b), and the difference between 2022 and 2019 (c). In (a) and (b), warmer colors indicate greater height and cooler colors indicate lower height. In (c), cooler colors indicate areas where canopy height decreased, and warmer colors indicate areas where canopy height increased. Detected and matched individual trees are symbolized as crosses (+) and are overlaid on all panes.

whether stand treatment objectives such as raising crown base height are met during prescribed burn activities.

6. Conclusions

Understanding how fire impacts mature tree growth is of critical importance for fire effects modeling and natural resource management, including planning and evaluation of prescribed fires and modeling growth and yield. This pilot study advances our understanding of fire effects by evaluating a multi-sensor methodology for assessing fire impacts on mature tree growth through the combined use of pre-, active-, and post-fire measurements. Our results highlight the utility of maximum FRPD for characterizing post-fire height growth in *Pinus ponderosa* and the potential for landscape-scale application (e.g., airborne and satellite derived FRP). The results of this study coupled with Sparks et al. (2018a) clearly demonstrate the utility of FRP_{max} as a scalable metric that can be used to broadly infer fire-induced impacts on post-fire growth in forested ecosystems. Further research could evaluate the potential integration of FRP_{max} based predictions of impacts to forest growth into Earth-system modeling frameworks assessing fire impacts on the global carbon cycle given synoptic scale assessments of fire emissions already use this metric (e.g., Kaiser et al., 2012). However, more research is warranted to assess this metric on non-coniferous forested systems. In terms of wider relevance to forestry, fire, and broader land management personnel, the measures of FRED and FRPD have been widely demonstrated to be related to fuel consumed and the emission of smoke and particulates in wildland fires (Wooster et al., 2021). Furthermore, FRPD is also related to the measure of Heat Release Rate (HRR) used within the Consume 4.2 submodule of Fuel and Fire Tools (FFT) software application that exports data to the Fire Emissions Prediction Simulator (FEPS), an application that is widely applied by forestry and land management personnel to predict pollutant emissions from wildland fires. As such, further research should evaluate the incorporation of FRPD datasets from field, aerial, and satellite sensor data within these existing wildland fire consumption and emission models, in addition to ecological effect models such as the First Order Fire Effects Model (FOFEM) (Lutes, 2020).

Although there was not significant support for using more integrative measures of heat flux, such as FRPDμ and FRED, to characterize post-fire tree growth, future research could evaluate these metrics on larger sample sizes and other tree size classes and species. Reduced height growth eight years post-fire highlights the persistence of fire effects and could be used to inform planning of prescribed fires and parameterization of fire effects models. This study used three ALS datasets to assess height change over time and supports the value of acquiring and using multitemporal ALS data to assess tree growth in areas affected by disturbances such as fire. Ultimately, the integrated pre-, active-, and post-fire data approach used here shows promise for furthering our understanding of how fire impacts tree structure and growth at multiple spatiotemporal scales.

CRediT authorship contribution statement

Aaron M. Sparks: Conceptualization, Methodology, Formal analysis, Writing – original draft. **Alistair M.S. Smith:** Methodology, Writing – review & editing. **Andrew T. Hudak:** Writing – review & editing. **Mark V. Corrao:** Writing – review & editing. **Robert L. Kremens:** Writing – review & editing. **Robert F. Keefe:** Writing – review & editing.

Declaration of Competing Interest

The authors declare the following financial interests/personal relationships which may be considered as potential competing interests: Mark Corrao reports a relationship with Northwest Management Incorporated that includes: employment.

Data availability

The authors do not have permission to share data.

Acknowledgements

The authors thank Northwest Management Incorporated (NMI, Moscow, Idaho) for providing the ALS datasets. We thank Z. Lyon and A. Argona for their assistance with field inventory data collection. We also thank the University of Idaho Experimental Forest staff and 21 students in the FOR 427 Prescribed Burning Laboratory class who assisted with planning and implementing the thinning and prescribed fire treatments. Partial funding for Sparks was provided by the National Institute of Food and Agriculture, USDA, McIntire Stennis project under IDAZ-ES-0609, and the Joint Fire Science Program under the GRIN award 16-2-01-09 and award 13-1-05-7. Smith was partially supported on the Agriculture and Food Research Initiative grant 2022-67021-37857 and by the National Science Foundation DMS award 1520873 and the Idaho Established Program to Stimulate Competitive Research award 1301792

and 2242769. This research was supported in part by the USDA Forest Service, Rocky Mountain Research Station. The findings and conclusions in this publication are those of the authors and should not be construed to represent any official USDA or U.S. Government determination or policy.

References

Abatzoglou, J.T., Battisti, D.S., Williams, A.P., Hansen, W.D., Harvey, B.J., Kolden, C.A., 2021. Projected increases in western US forest fire despite growing fuel constraints. Comm. Earth Environ. 2 (1), 1–8.

Alonzo, M., Morton, D.C., Cook, B.D., Andersen, H.-E., Babcock, C., Pattison, R., 2017. Patterns of canopy and surface layer consumption in a boreal forest fire from repeat airborne Lidar. Environ. Res. Lett. 12 (6), 065004.

Anderegg, W.R.L., Chegwidden, O.S., Badgley, G., Trugman, A., Cullenward, D., Abatzoglou, J.T., Hicke, J., Freeman, J., Hamman, J.J., Lawler, J., 2022. Future climate risks from stress, insects and fire across US forests. Ecol. Lett. 25 (6), 1510–1520.

Asner, G.P., Martin, R.E., Anderson, C.B., Knapp, D.E., 2015. Quantifying forest canopy traits: Imaging spectroscopy versus field survey. Remote Sens. Environ. 158, 15–27.

ASPRS, 2011. ASPRS LAS format standard 1.4. Available online: https://www.asprs.org/wp-content/uploads/2019/07/LAS_1_4_r15.pdf.

Bergmüller, K.O., Vanderwel, M.C., 2022. Predicting tree mortality using spectral indices derived from multispectral UAV imagery. Remote Sens. 14 (9), 2195.

Bowman, D.M.J.S., Williamson, G.J., Abatzoglou, J.T., Kolden, C.A., Cochrane, M.A., Smith, A.M.S., 2017. Human exposure and sensitivity to globally extreme wildfire events. Nature Ecol. Evol. 1 (3), 0058.

Bright, B.C., Hudak, A.T., McCarley, T.R., Spannuth, A., Sánchez-López, N., Ottmar, R.D., Soja, A.J., 2022. Multitemporal lidar captures heterogeneity in fuel loads and consumption on the Kaibab Plateau. Fire Ecol. 18 (1), 1–16.

Chasmer, L.E., Hopkinson, C.D., Petrone, R.M., Sitar, M., 2017. Using multitemporal and multispectral airborne lidar to assess depth of peat loss and correspondence with a new active normalized burn ratio for wildfires. Geophys. Res. Lett. 44 (23), 11–851.

Cheney, N.P., 1990. Quantifying bushfires. Math. Comp. Model. 13 (12), 9–15.

Cocke, A.E., Fulé, P.Z., Crouse, J.E., 2005. Comparison of burn severity assessments using Differenced Normalized Burn Ratio and ground data. Int. J. Wildland Fire 14 (2), 189–198.

Corrao, M.V., Sparks, A.M., Smith, A.M.S., 2022. A conventional cruise and felled-tree validation of individual tree diameter, height and volume derived from airborne laser scanning data of a Loblolly pine (P. taeda) stand in Eastern Texas. Remote Sens. 14 (11), 2567.

Falkowski, M.J., Smith, A.M.S., Gessler, P.E., Hudak, A.T., Vierling, L.A., Evans, J.S., 2008. The influence of conifer forest canopy cover on the accuracy of two individual tree measurement algorithms using lidar data. Canadian J. Remote Sens. 34, S338-S350.

Finney, M.A., Cohen, J.D., Forthofer, J.M., McAllister, S.S., Gollner, M.J., Gorham, D.J., Saito, K., Akafuah, N.K., Adam, B.A., English, J.D., 2015. Role of buoyant flame dynamics in wildfire spread. Proc. Nat. Acad. Sci. 112 (32), 9833–9838.

Freeborn, P.H., Wooster, M.J., Hao, W.M., Ryan, C.A., Nordgren, B.L., Baker, S.P., Ichoku, C., 2008. Relationships between energy release, fuel mass loss, and trace gas and aerosol emissions during laboratory biomass fires. J. Geophys. Res.: Atmos. 113 (D1).

Freeborn, P.H., Wooster, M.J., Roy, D.P., Cochrane, M.A., 2014. Quantification of MODIS fire radiative power (FRP) measurement uncertainty for use in satellite-based active fire characterization and biomass burning estimation. Geophys. Res. Lett. 41 (6), 1988–1994.

Furniss, T.J., Kane, V.R., Larson, A.J., Lutz, J.A., 2020. Detecting tree mortality with Landsat-derived spectral indices: Improving ecological accuracy by examining uncertainty. Remote Sens. Environ. 237, 111497.

Ganz, S., Käber, Y., Adler, P., 2019. Measuring tree height with remote sensing—A comparison of photogrammetric and LiDAR data with different field measurements. Forests 10 (8), 694.

Giglio, L., 2007. Characterization of the tropical diurnal fire cycle using VIRS and MODIS observations. Remote Sens. Environ. 108 (4), 407–421.

Giglio, L., Schroeder, W., Justice, C.O., 2016. The collection 6 MODIS active fire detection algorithm and fire products. Remote Sens. Environ. 178, 31–41.

Hamilton, D.A., Brothers, K.L., Jones, S.D., Colwell, J., Winters, J., 2021. Wildland fire tree mortality mapping from hyperspatial imagery using machine learning. Remote Sens. 13 (2), 290.

Harrington, C.A., Reukema, D.L., 1983. Initial shock and long-term stand development following thinning in a Douglas-fir plantation. Forest Sci. 29 (1), 33–46.

He, T., Pausas, J.G., Belcher, C.M., Schwilk, D.W., Lamont, B.B., 2012. Fire-adapted traits of Pinus arose in the fiery Cretaceous. New Phy. 194 (3), 751–759.

Hemingway, H., Kimsey, M., 2020. A multipoint felled-tree validation of height–age modeled growth rates. Forest Sci. 66 (3), 275–283.

Hessburg, P.F., Churchill, D.J., Larson, A.J., Haugo, R.D., Miller, C., Spies, T.A., North, M.P., Povak, N.A., Belote, R.T., Singleton, P.H., Gaines, W.L., Keane, R.E., Aplet, G.H., Stephens, S.L., Morgan, P., Bisson, P.A., Rieman, B.E., Salter, R.B., Reeves, G.H., 2015. Restoring fire-prone Inland Pacific landscapes: seven core principles. Landscape Ecol. 30 (10), 1805–1835.

Hiers, J.K., O'Brien, J.J., Varner, J.M., Butler, B.W., Dickinson, M., Furman, J., Gallagher, M., Godwin, D., Goodrick, S.L., Hood, S.M., Hudak, A., Kobziar, L.N., Linn, R., Loudermilk, E.L., McCaffrey, S., Robertson, K., Rowell, E.M., Skowronski, N., Watts, A.C., Yedinak, K.M., 2020. Prescribed fire science: The case for a refined research agenda. Fire Ecol. 16 (1).

Hood, S.M., Varner, J.M., Van Mantgem, P., Cansler, C.A., 2018. Fire and tree death: understanding and improving modeling of fire-induced tree mortality. Environ. Res. Lett. 13 (11), 113004.

Hudak, A.T., Strand, E.K., Vierling, L.A., Byrne, J.C., Eitel, J.U., Martinuzzi, S., Falkowski, M.J., 2012. Quantifying aboveground forest carbon pools and fluxes from repeat LiDAR surveys. Remote Sens. Environ. 123, 25–40.

Hudak, A.T., Dickinson, M.B., Bright, B.C., Kremens, R.L., Loudermilk, E.L., O'Brien, J.J., Hornsby, B.S., Ottmar, R.D., 2015. Measurements relating fire radiative energy density and surface fuel consumption–RxCADRE 2011 and 2012. Int. J. Wildland Fire 25 (1), 25–37.

Hyyppa, J., Inkinen, M., 1999. Detecting and estimating attributes for single tree using laser scanner. Photogramm. J. Finl. 16, 27–42.

Johnson, E.A., 1992. Fire and Vegetation Dynamics: Studies From the North American Boreal Forest. Cambridge University Press, New York.

Kaiser, J.W., Heil, A., Andreae, M.O., Benedetti, A., Chubarova, N., Jones, J., Morcrette, J.J., Razinger, M., Schultz, M.G., Suttie, M., van der Werf, G.R., 2012. Biomass burning emissions estimated with a global fire assimilation system based on observed fire radiative power. Biogeosciences 9, 527–554.

Keefe, R.F., Zimbelman, E.G., Picchi, G., 2022. Use of individual tree and product level data to improve operational forestry. Curr. Forestry Rep. 8 (2), 148–165.

Keeley, J.E., 2012. Ecology and evolution of pine life histories. Ann. For. Sci. 69 (4), 445–453.

Kolden, C.A., 2019. We're not doing enough prescribed fire in the Western United States to mitigate wildfire risk. Fire 2 (2), 30.

Kremens, R.L., Smith, A.M.S., Dickinson, M.B., 2010. Fire metrology: current and future directions in physics-based measurements. Fire Ecol. 6 (1), 13–35.

Kremens, R.L., Dickinson, M.B., Bova, A.S., 2012. Radiant flux density, energy density and fuel consumption in mixed-oak forest surface fires. Int. J. Wildland Fire 21 (6), 722–730.

Landsberg, J.D., Cochran, P.H., Finck, M.M., Martin, R.E. (1984) Foliar Nitrogen Content and Tree Growth After Prescribed Fire in Ponderosa Pine. USDA Forest Service, Pacific Northwest Research Station, Research Note PNW-412. (Ogden, UT).

Lee, D., Beuker, E., Viherä-Aarnio, A., Hynynen, J., 2021. Site index models with density effect for hybrid aspen (Populus tremula L.× P. tremuloides Michx.) plantations in southern Finland. Forest Ecol. Manag. 480, 118669.

Lefsky, M.A., Cohen, W.B., Acker, S.A., Parker, G.G., Spies, T.A., Harding, D., 1999. Lidar remote sensing of the canopy structure and biophysical properties of Douglas-fir western hemlock forests. Remote Sens. Environ. 70 (3), 339–361.

Lentile, L.B., Holden, Z.A., Smith, A.M.S., Falkowski, M.J., Hudak, A.T., Morgan, P., Lewis, S.A., Gessler, P.E., Benson, N.C., 2006. Remote sensing techniques to assess active fire characteristics and post-fire effects. Int. J. Wildland Fire 15 (3), 319–345.

Lutes, D. FOFEM 6.7 First Order Fire Effects Model User Guide, Fire and Aviation Management. Rocky Mountain Research Station Fire Modelling Institute, United States Department of Agriculture, 2020. Available online: https://www.firelab.org/project/fofem-fire-effects-model (accessed on 20 May 2023).

Lutz, J.A., Larson, A.J., Swanson, M.E., 2018. Advancing fire science with large forest plots and a long-term multidisciplinary approach. Fire 1 (1), 5.

Lutz, J.A., Struckman, S., Furniss, T.J., Cansler, C.A., Germain, S.J., Yocum, L.Y., McAvoy, D.J., Kolden, C.A., Smith, A.M.S., Swanson, M.E., Larson, A.J., 2020. Large-diameter trees dominate snag and surface biomass following reintroduced fire. Ecol. Process. 9 (1), 1–13.

Lyon, Z.D., Morgan, P., Stevens-Rumann, C.S., Sparks, A.M., Keefe, R.F., Smith, A.M.S., 2018. Fire behaviour in masticated forest fuels: lab and prescribed fire experiments. Int. J. Wildland Fire 27 (4), 280–292.

Ma, Q., Su, Y., Tao, S., Guo, Q., 2018. Quantifying individual tree growth and tree competition using bi-temporal airborne laser scanning data: a case study in the Sierra Nevada Mountains, California. Int. J. Digital Earth 11 (5), 485–503.

Mäkinen, H., Isomäki, A., 2004. Thinning intensity and growth of Scots pine stands in Finland. Forest Ecol. Manag. 201 (2–3), 311–325.

Martinuzzi, S., Vierling, L.A., Gould, W.A., Falkowski, M.J., Evans, J.S., Hudak, A.T., Vierling, K.T., 2009. Mapping snags and understory shrubs for a LiDAR-based assessment of wildlife habitat suitability. Remote Sens. Environ. 113 (12), 2533–2546.

Mathews, B.J., Strand, E.K., Smith, A.M.S., Hudak, A.T., Dickinson, B., Kremens, R.L., 2016. Laboratory experiments to estimate interception of infrared radiation by tree canopies. Int. J. Wildland Fire 25 (9), 1009–1014.

McCarley, T.R., Hudak, A.T., Restaino, J.C., Billmire, M., French, N.H., Ottmar, R.D., Hass, B., Zarzana, K., Goulden, T., Volkamer, R., 2022. A comparison of multitemporal airborne laser scanning data and the Fuel Characteristics Classification System for estimating fuel load and consumption. J. Geophys. Res.: Biogeosci. 127, e2021JG006733.

McCarley, T.R., Kolden, C.A., Vaillant, N.M., Hudak, A.T., Smith, A.M.S., Wing, B.M., Kellogg, B.S., Kreitler, J., 2017a. Multi-temporal LiDAR and Landsat quantification of fire-induced changes to forest structure. Remote Sens. Environ. 191, 419–432.

McCarley, T.R., Kolden, C.A., Vaillant, N.M., Hudak, A.T., Smith, A.M.S., Kreitler, J., 2017b. Landscape-scale quantification of fire-induced change in canopy cover following mountain pine beetle outbreak and timber harvest. Forest Ecol. Manag. 391, 164–175.

McCarley, T.R., Hudak, A.T., Sparks, A.M., Vaillant, N.M., Meddens, A.J.H., Trader, L., Mauro, F., Kreitler, J., Boschetti, L., 2020. Estimating wildfire fuel consumption with multitemporal airborne laser scanning data and demonstrating linkage with MODIS-derived fire radiative energy. Remote Sens. Environ. 251, 112114.

McDowell, N.G., Michaletz, S.T., Bennett, K.E., Solander, K.C., Xu, C., Maxwell, R.M., Middleton, R.S., 2018. Predicting chronic climate-driven disturbances and their mitigation. Trends Ecol. Evol. 33 (1), 15–27.
Meng, R., Wu, J., Zhao, F., Cook, B.D., Hanavan, R.P., Serbin, S.P., 2018. Measuring short-term post-fire forest recovery across a burn severity gradient in a mixed pine-oak forest using multi-sensor remote sensing techniques. Remote Sens. Environ. 210, 282–296.
Morgan, P., Keane, R.E., Dillon, G.K., Jain, T.B., Hudak, A.T., Karau, E.C., Sikkink, P.G., Holden, Z.A., Strand, E.K., 2014. Challenges of assessing fire and burn severity using field measures, remote sensing and modelling. Int. J. Wildland Fire 23 (8), 1045–1060.
Naesset, E., 1997. Estimating timber volume of forest stands using airborne laser scanner data. Remote Sens. Environ. 61 (2), 246–253.
NOAA, 2022. NOAA's US Climate Normals (1991-2020). NOAA National Centers for Environmental Information. Available online: https://www.ncei.noaa.gov/products/land-based-station/us-climate-normals (accessed November 29, 2022).
O'Brien, J.J., Hiers, J.K., Varner, J.M., Hoffman, C.M., Dickinson, M.B., Michaletz, S.T., Loudermilk, E.L., Butler, B.W., 2018. Advances in mechanistic approaches to quantifying biophysical fire effects. Curr. For. Rep. 4 (4), 161–177.
Partelli-Feltrin, R., Smith, A.M.S., Adams, H.D., Kolden, C.A., Johnson, D.M., 2021. Short-and long-term effects of fire on stem hydraulics in Pinus ponderosa saplings. Plant Cell Environ. 44 (3), 696–705.
Partelli-Feltrin, R., Smith, A.M.S., Adams, H.D., Thompson, R.A., Kolden, C.A., Yedinak, K.M., Johnson, D.M., 2023. Death from hunger or thirst? Phloem death, rather than xylem hydraulic failure, as a driver of fire-induced conifer mortality. New Phy. 237 (4), 1154–1163.
Picotte, J.J., Cansler, C.A., Koldem, C.A., Lutz, J.A., Key, C., Benson, N.C., Robertson, K. M., 2021. Determination of burn severity models ranging from regional to national scales for the conterminous United States. Remote Sens. Environ. 263, 112569.
Poorter, H., Niklas, K.J., Reich, P.B., Oleksyn, J., Poot, P., Mommer, L., 2012. Biomass allocation to leaves, stems and roots: meta-analyses of interspecific variation and environmental control. New Phy. 193 (1), 30–50.
Prichard, S.J., Hessburg, P.F., Hagmann, R.K., Povak, N.A., Dobrowski, S.Z., Hurteau, M. D., Kane, V.R., Keane, R.E., Kobziar, L.N., Kolden, C.A., North, M., Parks, S.A., Safford, H.D., Stevens, J.T., Yocom, L.L., Churchill, D.J., Gray, R.W., Huffman, D.W., Lake, F.K., Khatri-Chhetri, P., 2021. Adapting western North American forests to climate change and wildfires: 10 common questions. Ecol. App. 31 (8), e02433.
Qiu, H., Liu, S., Zhang, Y., Li, J., 2021. Variation in height-diameter allometry of ponderosa pine along competition, climate, and species diversity gradients in the western United States. For. Ecol. Manag. 497, 119477.
Rebain, S., 2015. The Fire and Fuels Extension to the Forest Vegetation Simulator: Updated Model Documentation; Internal Rep.; U.S. Department of Agriculture, Forest Service, Forest Management Service Center: Fort Collins, CO, USA.
Roy, D.P., Landmann, T., 2005. Characterizing the surface heterogeneity of fire effects using multi-temporal reflective wavelength data. Int. J. Remote Sens. 26 (19), 4197–4218.
Schroeder, W., Ellicott, E., Ichoku, C., Ellison, L., Dickinson, M.B., Ottmar, R.D., Clements, C., Hall, D., Ambrosia, V., Kremens, R., 2014a. Integrated active fire retrievals and biomass burning emissions using complementary near-coincident ground, airborne and spaceborne sensor data. Remote Sens. Environ. 140, 719–730.
Schroeder, W., Oliva, P., Giglio, L., Csiszar, I.A., 2014b. The New VIIRS 375 m active fire detection data product: Algorithm description and initial assessment. Remote Sens. Environ. 143, 85–96.
Sibona, E., Vitali, A., Meloni, F., Caffo, L., Dotta, A., Lingua, E., Motta, R., Garbarino, M., 2016. Direct measurement of tree height provides different results on the assessment of LiDAR accuracy. Forests 8 (1), 7.
Simonin, K., Kolb, T.E., Montes-Helu, M., Koch, G.W., 2006. Restoration thinning and influence of tree size and leaf area to sapwood area ratio on water relations of Pinus ponderosa. Tree Phys. 26 (4), 493–503.
Smith, A.M.S., Wooster, M.J., Drake, N.A., Dipotso, F.M., Falkowski, M.J., Hudak, A.T., 2005. Testing the potential of multi-spectral remote sensing for retrospectively estimating fire severity in African Savannahs. Remote Sens. Environ. 97 (1), 92–115.
Smith, A.M.S., Falkowski, M.J., Hudak, A.T., Evans, J.S., Robinson, A.P., Steele, C.M., 2009. A cross-comparison of field, spectral, and lidar estimates of forest canopy cover. Canadian J. Remote Sens. 35 (5), 447–459.
Smith, A.M.S., Sparks, A.M., Kolden, C.A., Abatzoglou, J.T., Talhelm, A.F., Johnson, D. M., Boschetti, L., Lutz, J.A., Apostol, K.G., Yedinak, K.M., Tinkham, W.T., Kremens, R.J., 2016. Towards a new paradigm in fire severity research using dose–response experiments. Int. J. Wildland Fire 25 (2), 158.
Smith, A.M.S., Talhelm, A.F., Johnson, D.M., Sparks, A.M., Kolden, C.A., Yedinak, K.M., Apostol, K.G., Tinkham, W.T., Abatzoglou, J.T., Lutz, J.A., Davis, A.S., Pregitzer, K. S., Adams, H.D., Kremens, R.L., 2017. Effects of fire radiative energy density dose on Pinus contorta and Larix occidentalis seedling physiology and mortality. Int. J. Wildland Fire 26 (1), 82.
Sparks, A.M., Kolden, C.A., Talhelm, A.F., Smith, A.M.S., Apostol, K.G., Johnson, D.M., Boschetti, L., 2016. Spectral indices accurately quantify changes in seedling physiology following fire: towards mechanistic assessments of post-fire carbon cycling. Remote Sens. 8 (7), 572.
Sparks, A.M., Smith, A.M.S., Talhelm, A.F., Kolden, C.A., Yedinak, K.M., Johnson, D.M., 2017. Impacts of fire radiative flux on mature Pinus ponderosa growth and vulnerability to secondary mortality agents. Int. J. Wildland Fire 26 (1), 95–106.
Sparks, A.M., Kolden, C.A., Smith, A.M.S., Boschetti, L., Johnson, D.M., Cochrane, M.A., 2018a. Fire intensity impacts on post-fire temperate coniferous forest net primary productivity. Biogeosciences 15 (4), 1173–1183.
Sparks, A.M., Talhelm, A.F., Feltrin, R.P., Smith, A.M.S., Johnson, D.M., Kolden, C.A., Boschetti, L., 2018b. An experimental assessment of the impact of drought and fire on western larch injury, mortality and recovery. Int. J. Wildland Fire 27 (7), 490–497.
Sparks, A.M., Corrao, M.V., Smith, A.M.S., 2022. Cross-comparison of individual tree detection methods using low and high pulse density airborne laser scanning data. Remote Sens. 14 (14), 3480.
Sparks, A.M., Blanco, A.S., Wilson, D.R., Schwilk, D.W., Johnson, D.M., Adams, H.D., Bowman, D.M., Hardman, D.D. and Smith, A.M., 2023. Fire intensity impacts on physiological performance and mortality in Pinus monticola and Pseudotsuga menziesii saplings: A dose–response analysis. Tree Phys. tpad051.
Sparks, A.M., Smith, A.M.S., 2022. Accuracy of a lidar-based individual tree detection and attribute measurement algorithm developed to inform forest products supply chain and resource management. Forests 13 (1), 3.
Starker, T., 1934. Fire Resistance in the Forest. J. Forest 32, 462–467.
Steady, W.D., Partelli Feltrin, R., Johnson, D.M., Sparks, A.M., Kolden, C.A., Talhelm, A. F., Lutz, J.A., Boschetti, L., Hudak, A.T., Nelson, A.S., Smith, A.M.S., 2019. The survival of Pinus ponderosa saplings subjected to increasing levels of fire behavior and impacts on post-fire growth. Fire 2 (2), 23.
Tymińska-Czabańska, L., Hawryło, P., Socha, J., 2022. Assessment of the effect of stand density on the height growth of Scots pine using repeated ALS data. Int. J. Appl. Earth Obs. Geoinform. 108, 102763.
United States Geological Survey. Lidar Base Specification Version 2.1. 2019. Available online: https://www.usgs.gov/3DEP/lidarspec (accessed on December 2, 2023).
VanderWeide, B.L., Hartnett, D.C., 2011. Fire resistance of tree species explains historical gallery forest community composition. Forest Ecol. Manage. 261 (9), 1530–1538.
Wang, Y., Lehtomäki, M., Liang, X., Pyörälä, J., Kukko, A., Jaakkola, A., Liu, J., Feng, Z., Chen, R., Hyyppä, J., 2019. Is field-measured tree height as reliable as believed–A comparison study of tree height estimates from field measurement, airborne laser scanning and terrestrial laser scanning in a boreal forest. ISPRS J. Photogramm. Remote Sens. 147, 132–145.
Wooster, M.J., Roberts, G.J., Giglio, L., Roy, D.P., Freeborn, P.H., Boschetti, L., Justice, C., Ichoku, C., Schroeder, W., Davies, D., Smith, A.M.S., Setzer, A., Csiszar, I., Strydom, T., Frost, P., Zhang, T., Xu, W., de Jong, M.C., Johnston, J.M., Ellison, L., Vadrevu, K., Sparks, A.M., Nguyen, H., McCarty, J., Tanpipat, V., Schmidt, C., San-Miguel-Ayanz, J., 2021. Satellite remote sensing of active fires: History and current status, applications and future requirements. Remote Sens. Environ. 267, 112694.
Wulder, M.A., White, J.C., Alvarez, F., Han, T., Rogan, J., Hawkes, B., 2009. Characterizing boreal forest wildfire with multi-temporal Landsat and LIDAR data. Remote Sens. Environ. 113 (7), 1540–1555.
Yu, X., Hyyppä, J., Kaartinen, H., Maltamo, M., 2004. Automatic detection of harvested trees and determination of forest growth using airborne laser scanning. Remote Sens. Environ. 90 (4), 451–462.
Zhao, K., Suarez, J.C., Garcia, M., Hu, T., Wang, C., Londo, A., 2018. Utility of multitemporal lidar for forest and carbon monitoring: Tree growth, biomass dynamics, and carbon flux. Remote Sens. Environ. 204, 883–897.